Spectral and polarization properties of ‘cholesteric liquid crystal – phase plate – metal’ structure

S. Ya. Vetrov[1,2], M. V. Pyatnov[2], and I. V. Timofeev[1,3]

[1]*L.V. Kirensky Institute of Physics, Siberian Branch of the Russian Academy of Sciences, Krasnoyarsk 660036, Russia*
[2]*Institute of Engineering Physics and Radio Electronics, Siberian Federal University, Krasnoyarsk 660041, Russia*
[3]*Laboratory for Nonlinear Optics and Spectroscopy, Siberian Federal University, Krasnoyarsk 660041, Russia*

Email: MaksPyatnov@yandex.ru

Abstract

We investigate the localized surface modes in a structure consisting of the cholesteric liquid crystal layer, a phase plate, and a metal layer. These modes are analogous to the optical Tamm states. The nonreciprocal transmission of polarized light propagating the forward and backward directions is established. It is demonstrated that the transmission spectrum can be controlled by external fields acting on the cholesteric and by varying the plane of polarization of the incident light.

Keywords: photonic band gap materials, cholesteric liquid crystals, localized states, optical filters, optical waveguides

1. Introduction

The surface electromagnetic states in photonic-crystal structures have been attracting attention of researches for a long time [1]. In recent years, there has been an increased interest in a special type of the localized electromagnetic states excited at the normal incident that are called the optical Tamm states (OTSs) [2]. Such states are analogous to the Tamm surface states in physics of condensed matter. They can be excited between two different photonic crystals with overlapping band gaps [3] or between a photonic crystal and a medium with negative permittivity ε [4, 5]. In experiments, the OTS manifests itself as a narrow peak in the transmission spectrum of a sample [6, 7].

The surface modes and OTSs are promising for application in sensors and optical switches [8], multichannel filters [9], Faraday- and Kerr-effect amplifiers [7, 10], organic solar cells [11], and absorbers [12]. The authors of study [13] experimentally demonstrated a laser based on the Tamm structure consisting of quantum wells embedded in a Bragg reflector with the silver-coated surface. Gazzano et al. experimentally showed the

possibility of implementation of a single-photon source on the basis of confined Tamm plasmon modes [14]. The optical Tamm states in magnetophotonic crystals were investigated in studies [7, 15−17]. The hybrid states were studied in [18−21]. In [22], the electro-optically tunable Tamm plasmon exciton polaritons were investigated. The authors of [23] predicted that the edges of a finite one-dimensional array of dielectric nanoparticles with the high refractive index can support evanescent OTSs.

The authors of [24] proposed and implemented the extremely high-efficiency transmission of light through a nanohole in a gold film, which was placed in the light field localized at the interface between the film and a one-dimensional photonic crystal. This effect is related to the field amplification at the interface between the superlattice and the metal film due to the occurrence of the OTS.

An important problem of optoelectronics is fabrication of materials with the spectral properties controlled by external factors. A special class of one-dimensional photonic crystals is formed by cholesteric liquid crystals (CLCs), which have unique properties: a wide passband, strong nonlinearity, and high sensitivity to external fields [25, 26]. By varying temperature and pressure and by applying electromagnetic fields and mechanical stresses, one can, e.g., vary the cholesteric helix pitch and, consequently, the band gap position. A qualitative difference of CLCs from other kinds of photonic crystals (PCs) is that their diffraction reflectivity is selective to polarization. The circularly polarized light propagating along the helix normal with the polarization direction coinciding with the direction of rotation of the CLC experiences Bragg reflection. The Bragg reflection occurs in the wavelength range between $\lambda_1 = pn_o$ and $\lambda_2 = pn_e$, where p is the helix pitch and n_o and n_e are the ordinary and extraordinary refractive indices of the CLC, respectively. This circular polarization is called diffracting. Light with the opposite circular polarization does not experience the Bragg reflection. This polarization is called nondiffracting.

In our previous study [27], we demonstrated the possibility of implementation of localized surface states in a structure with the CLC. These states are analogous to the OTSs for scalar structures. We failed to obtain the surface state at the CLC/metal interface at the normal incidence of light. The difficulty consists in the wave polarization change upon reflection from a metal and in the existence of Bragg reflection for a certain polarization. To localize light, it is necessary to change the wave phase between the CLC and metal. To do so, we proposed to use a quarter-wave phase plate.

In this study, we continue investigations of the properties of OTSs in the system with a CLC. We demonstrate the effects that take place during propagation of light in the backward direction. We investigate the transmission spectra upon variation in the CLC helix pitch and calculate the transmission spectra for the linearly polarized radiation.

2. Model description and determination of transmission

The investigated structure consists of a thin right-hand CLC layer, a quarter-wave anisotropic plate, and a metal film (figure 1). The plate is cut parallel to the optical axis and shifts the wave phase by π/2. At the interface between the CLC and the phase plate, the cholesteric director, i.e., the preferred direction of molecules, is oriented along the optical axis. The CLC layer thickness is L = 2 μm, the helix pitch is p = 0.4 μm, and the ordinary and extraordinary refractive indices are n_o=1.4 and n_e=1.6, respectively. The phase plate thickness is d = 0.75 μm and its refractive indices are $n'_o=n_o$ and $n'_e=n_e$. The parameters of the phase plate satisfy the relation

$$2\pi(n'_e-n'_o)d/\lambda=\pi/2 \tag{1}$$

The phase plate is coupled with a silver film with the thickness d_m = 50 nm. The permittivity of the metal is specified in the form of the Drude approximation

$$\varepsilon(\omega)=\varepsilon_0-\frac{\omega_p^{\,2}}{\omega(\omega+i\gamma)}, \tag{2}$$

where ε_0 = 5 is the constant that takes into account the contribution of interband transitions of bound electrons, $\hbar\omega_p$ = 9 eV is the plasma frequency, and $\hbar\gamma$ = 0.02 eV is the reciprocal electron relaxation time [28]. The structure is surrounded by a medium with the refractive index n equal to the average refractive index of CLC.

The optical properties and field distribution in the structure were numerically analyzed with the use of a 4x4 Berreman transfer matrix at the normal incidence of light on the sample [17, 18]. The equation describing the propagation of light with frequency ω along the z axis of the cholesteric is

$$\frac{d\Psi}{dz}=\frac{i\omega}{c}\Delta(z)\Psi(z), \tag{3}$$

where $\Psi(z)=(E_x,H_y,E_y,-H_x)^T$ and $\Delta(z)$ is the Berreman matrix, which depends on the dielectric function and the incident wave vector.

3. Results and discussion

3.1. Optical localized states

In the paper [27] the transmission spectrum of the structure under consideration was shown. Fig. 2a shows the maximal transmittance at a wavelength corresponding to localized state at different values of the thickness of the metal d_m. The inset shows the transmission spectrum of the CLC and the entire structure at d_m = 50 nm. The Bragg reflection region lies between 560 and 640 nm. At these wavelengths, the real part of the permittivity of silver is negative. At the wavelength corresponding to the CLC band gap, a narrow transmission peak is observed. The electric field intensity distribution in the sample for the diffracting polarization is illustrated in figure 2b. The light is localized near the metal film with the maximum electric field value at the interface between the phase plate and metal. The decay of the localized mode field in the metal is caused by the negative permittivity of the metal film, while the decay of this field in the CLC is caused by Bragg reflection at the CLC/plate interface.

Let us consider the occurrence of localization between the CLC and the metal (figure 3). First, we explain why the light cannot be localized between the CLC and the metal without the quarter-wave phase plate.

We will investigate the four cases:

(i) The left-hand circularly polarized light enters the CLC and freely passes through it. Upon reflection from the metal, the left-hand circular polarization transforms to the right-hand one. Upon reflection from the CLC, the right-hand circular polarization is retained. Upon repeated reflection from the metal, the right-hand circular polarization transforms to the left-hand one and the light propagates through the crystal in the backward direction (figure 3a).

(ii) The right-hand diffracting-polarized light enters the CLC. A part of the light passed through the CLC retains its polarization, but upon reflection from the metal the right-hand circular polarization transforms to the left-hand one and the light freely passes through the CLC structure in the backward direction (figure 3b).

Let us consider the effect of the quarter-wave plate on the polarization of light.

(iii) The left-hand circularly polarized light enters the CLC. The light freely passes through the CLC. The light passed through the plate acquires the linear polarization. Upon reflection from the metal, the linear polarization is retained. The light passed through the plate in the backward direction acquires the left-hand circular polarization. After that, the light propagates through the CLC in the backward direction (figure 3c).

(iv) The right-hand diffracting-polarized light enters the CLC. A part of the light passed through the CLC retains its polarization. The light passed through the plate acquires the linear polarization. Upon reflection from the metal, the linear polarization is retained. The light passed through the plate in the backward direction acquires

the right-hand circular polarization. Upon repeated reflection from the CLC, the light retains its right-hand circular polarization (figure 3d). Thus, the light is localized between the CLC and the metal.

3.2. Transmission nonreciprocity

For a long time, the cholesteric liquid crystals have been attracting attention of researchers that want to effectively manipulate by light. One of the promising effects in the structures consisting of the CLCs and anisotropic elements is the different transmission spectra for the light of a certain polarization propagating in the forward and backward directions. This phenomenon was demonstrated, in particular, by Hwang et al. [31]. The authors proposed the electric-field-tunable optical diode based on two identically twisted CLCs separated by the nematic liquid crystal layer. As a result, the transmission spectra for the diffracting-polarized light propagating in the forward and backward directions were qualitatively different.

We established that the analogous effect takes place in the investigated model. Figure 4 presents the transmission spectra of the structure at the wave incidence on the CLC and on the metal film for the right- and left-hand circularly polarized light. When the light with the diffracting polarization propagates in the forward direction, the transmittance is 0.57; when the light propagates in the backward direction, the transmittance is 0.34. Thus, we deal with the transmission nonreciprocity. It was observed that when the left-hand circularly polarized light enters the structure, the spectrum changes. The transmittances in the forward and backward directions are 0.09 and 0.32, respectively. It should be noted that this effect cannot be implemented in scalar structures.

To elucidate the origin of this effect, we consider the light polarization dynamics at the incidence on the CLC (figures 5a and 5b) and on the metal (figures 5c and 5d).

When the light with the right-hand diffracting polarization enters the CLC, a part of the light passed through the crystal approximately retains its polarization at the CLC output. After passing through the quarter-wave plate, the light acquires the linear polarization. The unabsorbed part of light leaves the metal. Upon reflection from the metal, the linear polarization is retained. After passing through the metal in the backward direction, the light acquires the right-hand circular polarization. Upon repeated reflection from the CLC, the light retains its right-hand circular polarization. Again, the linearly polarized light leaves the metal (figure 5a).

For the backward incidence of light (figure 5c), the situation is qualitatively different. It appears that a half of light unabsorbed by the metal and unreflected from it, is reflected from the cholesteric due to the linear polarization.

The situation is similar at the nondiffracting left-hand polarization (figures 5b and 5d). Since at the incidence of light on the metal the light of the both circular polarizations propagates similarly, we can expect that the transmittances corresponding to the OTSs for the left- and right-hand polarizations will almost coincide, which was confirmed by the calculations (figure 4).

The structure under study can be used as a polarization optical diode. The advantages of this optical diode are its tunability and manufacturability, since it consists of only three elements.

3.3. Controlling the transmission spectrum of the structure

In contrast to the case of scalar structures, the transmission spectra of the CLCs can be easily and effectively controlled, because the transmission spectra of the CLCs are different for different polarizations and the helix pitch of the entire CLC or its part can be changed by an external field [32, 33, 34]. The change in the CLC helix pitch will lead to the change in the position of the Bragg reflection region in the crystal.

As was shown in [27], the localized mode is excited in the sample by light of different polarizations, which though make different contributions to the excitation. This effect is explained by the fact that light of the both circular polarizations excites a localized mode by transforming the polarizations at the dielectric interfaces. As a result, any polarization of light becomes elliptic, to different extents, at the CLC output, depending on the initial polarization and crystal thickness.

In this study, we investigated transmission of the linearly polarized light by the structure. It was established that the transmittance of the structure at the frequency corresponding to the OTS depends on angle φ between the optical axis of the phase plate and the polarization plane of polarization of the incident linearly polarized light (figure 6a).

It can be seen from the plots that the transmission maxima at the propagation of light in the forward and backward directions are shifted relative to each other. For the backward incidence of light, the transmittance of the structure is maximum at an angle of 45^0 between the plane of polarization of the incident light and the optical axis of the phase plate. This is caused by transformation of the linear polarization to the circular one during propagation of light through the quarter-wave phase plate. Consequently, all the light that reaches the CLC will pass through it.

Figure 6b shows the dependence of the maximum squared absolute value of the electric field for different angles φ. Using this dependence, one can determine the polarization at which the radiation is the most effectively

localized in the system. It can be seen that the localization at the frequency corresponding to the localized state at the light incidence on the CLC multiply exceeds that at the light incidence on the metal film.

As was mentioned above, an important advantage of the CLC over other photonic crystals is the high sensitivity of the former to external fields. Varying the parameters of the system, we can control the position of the transmission peak corresponding to the OTS. The stronger temperature or applied voltage dependences of the helix pitch as compared to the analogous dependences of other structure elements can be used for effective controlling the frequency of the transmission peak related to light tunneling through the localized state (figure 7).

4. Conclusions

We demonstrated the existence of the surface states similar to the OTSs localized in the structure that contains a cholesteric liquid crystal and a silver layer. The wave polarization variation upon reflection from the metal and special polarization properties of the CLC makes us introduce the anisotropic quarter-wave element between the cholesteric and metal layers. The origin of light localization in the investigated system was explained in detail.

It is difficult to form a direct contact between the CLC and the metal. To do so, one should apply orientants in the form of layers of an anisotropic material. The orientant can simultaneously be a quarter-wave phase plate. Varying the thickness of this plate, one can implement the localized state.

We showed that the transmission spectra for the light propagating in the forward and backward direction are different; i.e., we deal with the transmission nonreciprocity. Therefore, the investigated structure can be used as a polarization optical diode based on surface photonic modes.

We demonstrated that the transmission spectrum of such a system can be effectively controlled. At any polarization of the incident wave, the light is localized with the maximum field intensity at the interface between the plate and the metal. However, different ellipticities of the waves passed through the CLC and their polarization properties lead to different transmittances for each polarization.

Varying the plane of polarization of the linearly polarized incident radiation, one can easily change the transmittance at the wavelength corresponding to the localized state. We studied the dependence of the transmission maxima on the angle between the optical axis of the phase plate and the plane of polarization of the incident light. Using this dependence, we determined the angles at which the transmission of the system is maximum. It was found that the forward light localizes stronger than the backward one.

We showed that the transmission peak position can be controlled by varying the CLC helix pitch with the use of external fields.

To sum up, note that the observed surface state is, in fact, the eigenmode of the microcavity with the CLC layers and metal plane working as mirrors. Consequently, it becomes possible to induce laser generation in a microcavity by using the phase plate from an optically active material.

Acknowledgments

This work was supported by the Russian Foundation for Basic Research, project no. 14-02-31248 and the Ministry of Education and Science of the Russian Federation, Government program, project no. 3.1276.2014/K.

References

1. Vinogradov A P, Dorofeenko A V, Merzlikin A M and Lisyansky A A 2010 Surface states in photonic crystals *Phys. Usp.* **53** 243–56
2. Kavokin A, Shelykh I and Malpuech G 2005 Optical Tamm states for the fabrication of polariton lasers *Appl. Phys. Lett.* **87** 261105
3. Kavokin A V, Shelykh I A and Malpuech G 2005 Lossless interface modes at the boundary between two periodic dielectric structures *Phys. Rev. B* **72** 233102
4. Kaliteevski M, Iorsh I, Brand S, Abram R A, Chamberlain J M, Kavokin A V and Shelykh I A 2007 Tamm plasmon-polaritons: Possible electromagnetic states at the interface of a metal and a dielectric Bragg mirror *Phys. Rev. B* **76** 165415
5. Vetrov S Ya, Bikbaev R G and Timofeev I V 2013 Optical Tamm States at the Interface between a Photonic Crystal and a Nanocomposite with Resonance Dispersion *JETP* **117** 988-98
6. Sasin M E, Seisyan R P, Kalitteevski M A, Brand S, Abram R A, Chamberlain J M, Egorov A Yu, Vasil'ev A P, Mikhrin V S and Kavokin A V 2008 Tamm plasmon polaritons: Slow and spatially compact light *Appl. Phys. Lett.* **92**, 251112
7. Goto T, Dorofeenko A V, Merzlikin A M, Baryshev A V, Vinogradov A P, Inoue M, Lisyansky A A and Granovsky A B 2008 Optical Tamm States in One-Dimensional Magnetophotonic Structures *Phys. Rev. Lett.* **101** 113902
8. Zhang W L and Yu S F 2010 Bistable switching using an optical Tamm cavity with a Kerr medium *Opt. Commun.* **283** 2622-6

9. Zhou H, Yang G, Wang K, Long H and Lu P 2010 Multiple optical Tamm states at a metal–dielectric mirror interface *Opt. Lett.* **35** 4112-4
10. Vinogradov A P, Dorofeenko A V, Erokhin S G, Inoue M, Lisyansky A A, Merzlikin A M and Granovsky A B 2006 Surface state peculiarities in one-dimensional photonic crystal interfaces *Phys. Rev. B* **74** 045128
11. Zhang X-L, Song J-F, Li X-B, Feng J and Sun H-B 2012 Optical Tamm states enhanced broad-band absorption of organic solar cells *Appl. Phys. Lett.***101** 243901
12. Gong Y, Liu X, Lu H, Wang L and Wang G 2011 Perfect absorber supported by optical Tamm states in plasmonic waveguide *Opt. Exp.* **19** 18393-8
13. Symonds C, Lheureux G, Hugonin J P, Greffet J J, Laverdant J, Brucoli G, Lemaitre A, Senellart P and Bellessa J 2013 Confined Tamm Plasmon Lasers *Nano. Lett.* **13** 3179-84
14. Gazzano O, Michaelis de Vasconcellos S, Gauthron K, Symonds C, Voisin P, Bellessa J, Lemaıˆtre A and Senellart P 2012 Single photon source using confined Tamm plasmon modes *Appl. Phys. Lett.* **100** 232111
15. Dong H Y, Wang J and Cui T J 2013 One-way Tamm plasmon polaritons at the interface between magnetophotonic crystals and conducting metal oxides *Phys. Rev. B* **87** 045406
16. Da H, Bao Q, Sanaei R, Teng J, Loh K P, Garcia-Vidal F J and Qiu C-W 2013 Monolayer graphene photonic metastructures: Giant Faraday rotation and nearly perfect transmission *Phys. Rev. B* **88** 205405
17. Khokhlov N E, Prokopov A R, Shaposhnikov A N, Berzhansky V N, Kozhaev M A, Andreev S N, Ravishankar Ajith P, Achanta Venu Gopal, Bykov D A, Zvezdin A K and Belotelov V I 2015 Photonic crystals with plasmonic patterns: novel type of the heterostructures for enhanced magneto-optical activity *J. Phys. D: Appl. Phys.* **48** 095001
18. Kaliteevski M, Brand S, Abram R A, Iorsh I, Kavokin A V and Shelykh I A 2009 Hybrid states of Tamm plasmons and exciton polaritons *Appl. Phys. Lett.* **95** 251108
19. Brückner R, Sudzius M, Hintschich S I, Fröb H, Lyssenko V G, Kaliteevski M A, Iorsh I, Abram R A, Kavokin A V and Leo K 2012 Parabolic polarization splitting of Tamm states in a metal-organic microcavity *Appl. Phys. Lett.* **100** 062101
20. Afinogenov B I, Bessonov V O, Nikulin A A and Fedyanin A A 2013 Observation of hybrid state of Tamm and surface plasmon-polaritons in one-dimensional photonic crystals *Appl. Phys. Lett.* **103** 061112
21. Kaliteevski M A and Lazarenko A A 2013 Reduced absorption of light by metallic intra-cavity contacts: Tamm plasmon based laser mode engineering *Tech. Phys. Lett.* **39** 698-701

22. Gessler J, Baumann V, Emmerling M, Amthor M, Winkler K, Höfling S, Schneider C, and Kamp M 2014 Electro optical tuning of Tamm-plasmon exciton-polaritons *Appl. Phys. Lett.* **105** 181107
23. Savelev R S, Miroshnichenko A E, Sukhorukov A A, Kivshar Y S 2014 Optical Tamm states in arrays of all-dielectric nanoparticles *JETP Letters* **100** 430–3
24. Treshin I V, Klimov V V, Melentiev P N and Balykin V I 2013 Optical Tamm state and extraordinary light transmission through a nanoaperture *Phys. Rev. A* **88** 023832
25. Belyakov V A 1992 *Diffraction Optics of Complex Structured Periodic Media* (New York: Springer Verlag)
26. Blinov L M 2011 *Structure and Properties of Liquid Crystals* (Dordrecht Heidelberg London New York: Springer) chap 12
27. Vetrov S Y, Pyatnov M V and Timofeev I V 2014 Surface modes in "photonic cholesteric liquid crystal–phase plate–metal" structure *Opt. Lett.* **39** 2743–6
28. Johnson P B and Christy R W 1972 Optical Constants of the Noble Metals *Phys. Rev. B* **6** 4370–9
29. Berreman D W 1972 Optics in Stratified and Anisotropic Media: 4 X 4-Matrix Formulation *J. Opt. Soc. Am.* **62** 502–10
30. Palto S P 2001 An algorithm for solving the optical problem for stratified anisotropic media *JETP* **92** 552–60
31. Hwang J, Song M H, Park B, Nishimura S, Toyooka T, Wu J W, Takanishi Y, Ishikawa K and Takezoe H 2005 Defect mode lasing from a double-layered dye-doped polymeric cholesteric liquid crystal films with a thin rubbed defect layer *Nat. Mat*. **4** 383–6
32. Dolganov P V, Ksyonz G S, Dolganov V K 2013 Photonic liquid crystals: Optical properties and their dependence on light polarization and temperature *Phys. Solid State* **55** 1101–4
33. Rodarte A L, Cisneros F, Hirst Linda S and Ghosh S 2014 Dye-integrated cholesteric photonic luminescent solar concentrator *Liquid Crystals* **41** 1442–7
34. Hsiao Y-C, Wang H-T and Lee W 2014 Thermodielectric generation of defect modes in a photonic liquid crystal *Opt. Express* **22** 3593–9

Figure Captions

Figure 1. Schematic of the CLC layer−phase plate−metal layer structure.

Figure 2. (a) Transmission coefficients at a wavelength corresponding to localized state (λ = 586 nm) for different values of the thickness of the metal film d_m. The inset shows the transmission spectrum of a cholesteric liquid crystal (dashed line), and the entire structure (solid line) with d_m = 50 nm. (b) Spatial distribution of the field local intensity in the sample normalized to the input value for three values of d_m (λ=586 nm).

Figure 3. Localization of light for right-hand (R) and left-hand (L) polarizations in the structures consisting of (a, b) the CLC and metal layers and (c, d) the CLC layer, phase plate, and metal layer.

Figure 4. Transmission spectrum of the structure for incident waves with (a) the right-hand and (b) left-hand circular polarization. Solid line corresponds to the forward incidence on the CLC and dashed line, to the backward incidence on the metal.

Figure 5. Light polarization dynamics at the incidence (a, b) on the CLC and (c, d) on the metal. R and L are the right- and left-hand circular polarization and “linear” is the linear polarization.

Figure 6. (a) Transmittances corresponding to the localized state at different φ for the light incident on the CLC (solid line) and on the metal (dashed line). (b) Electric field intensity at the phase plate - metal interface at different φ for the light incident on the CLC (solid line) and on the metal (dashed line).

Figure 7. Transmission spectrum of the structure versus cholesteric helix pitch.

Figures

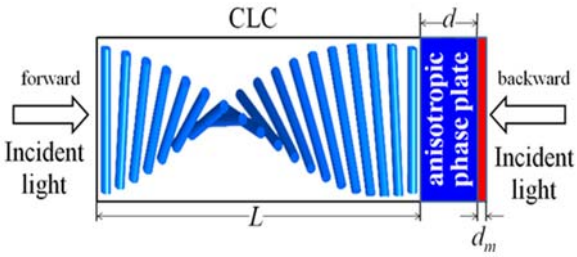

Figure 1. Schematic of the CLC layer−phase plate−metal layer structure.

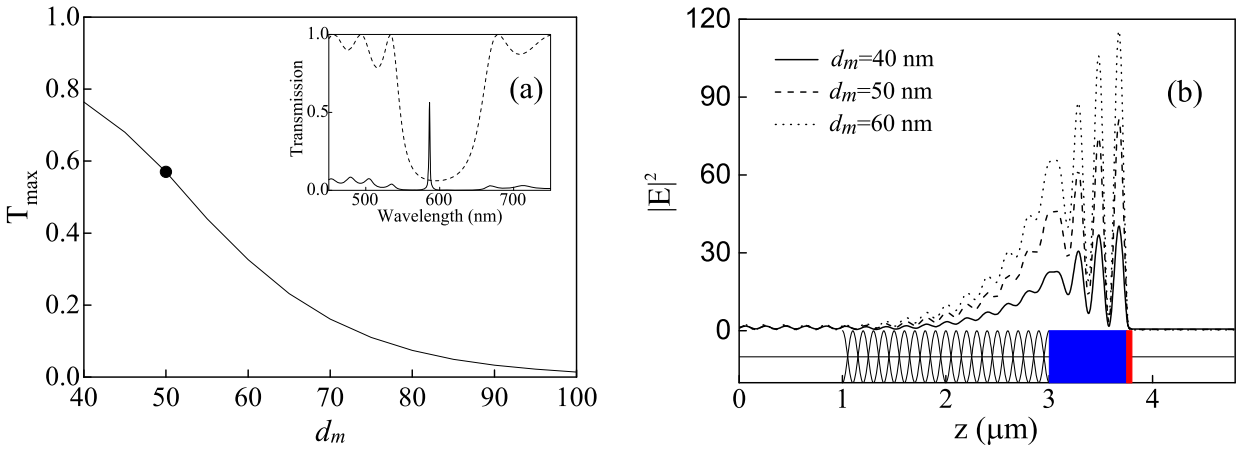

Figure 2. (a) Transmission coefficients at a wavelength corresponding to localized state (λ = 586 nm) for different values of the thickness of the metal film d_m. The inset shows the transmission spectrum of a cholesteric liquid crystal (dashed line), and the entire structure (solid line) with d_m = 50 nm. (b) Spatial distribution of the field local intensity in the sample normalized to the input value for three values of d_m (λ=586 nm).

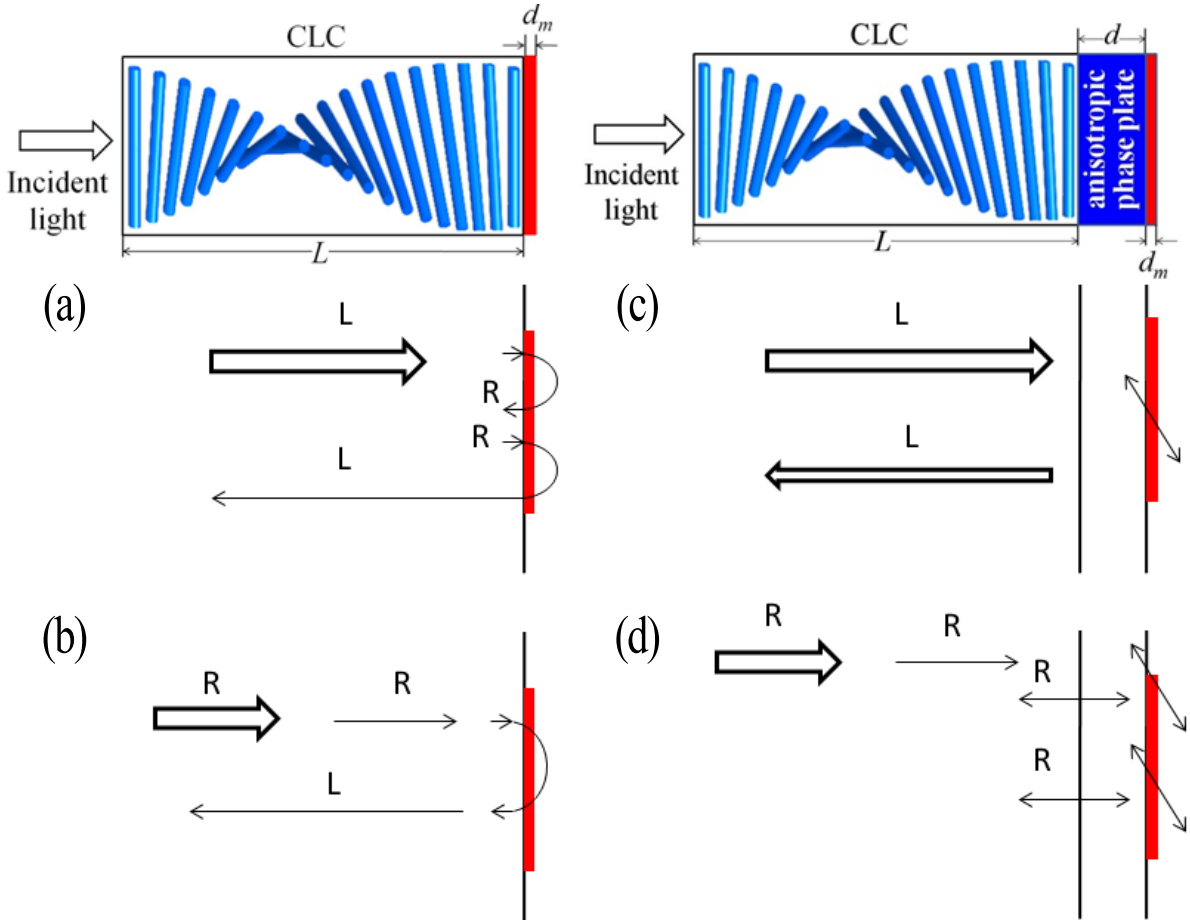

Figure 3. Localization of light for right-hand (R) and left-hand (L) polarizations in the structures consisting of (a, b) the CLC and metal layers and (c, d) the CLC layer, phase plate, and metal layer.

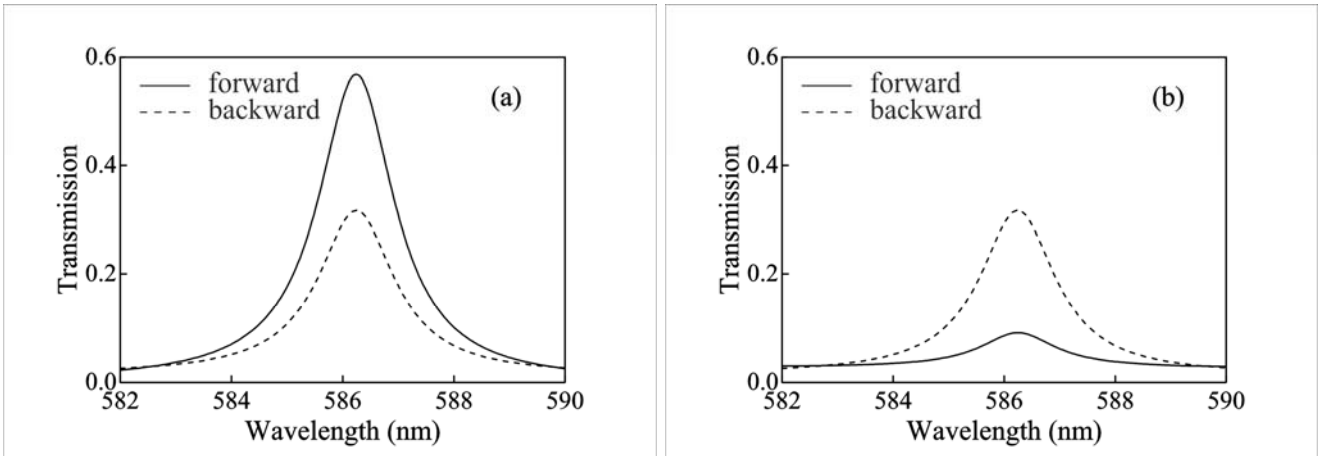

Figure 4. Transmission spectrum of the structure for incident waves with (a) the right-hand and (b) left-hand circular polarization. Solid line corresponds to the forward incidence on the CLC and dashed line, to the backward incidence on the metal.

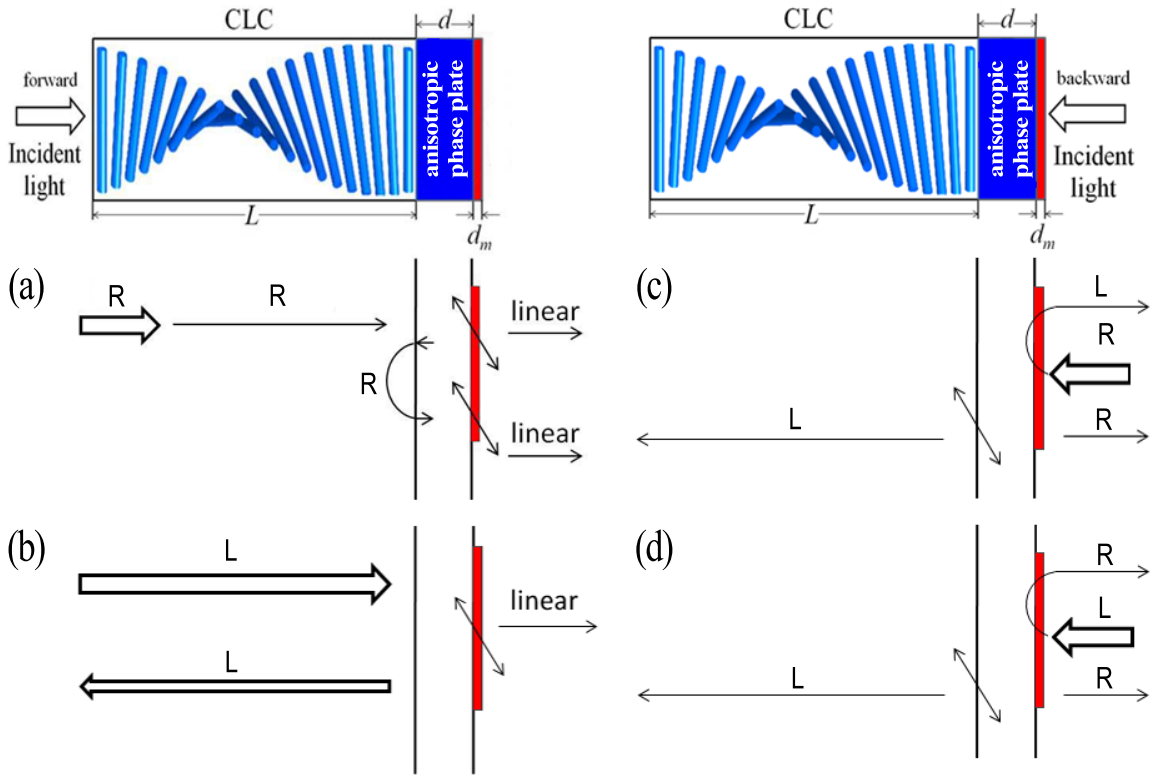

Figure 5. Light polarization dynamics at the incidence (a, b) on the CLC and (c, d) on the metal. R and L are the right- and left-hand circular polarization and "linear" is the linear polarization.

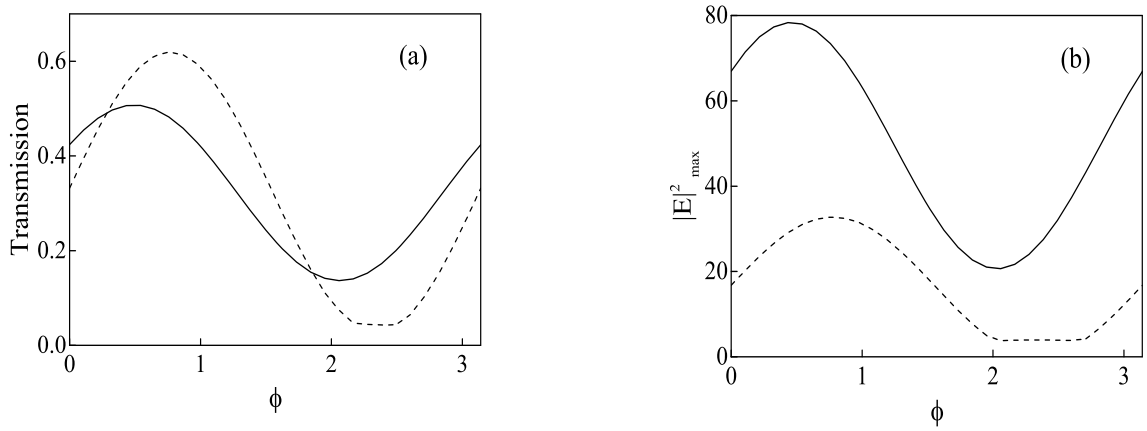

Figure 6. (a) Transmittances corresponding to the localized state at different φ for the light incident on the CLC (solid line) and on the metal (dashed line). (b) Electric field intensity at the phase plate – metal interface at different φ for the light incident on the CLC (solid line) and on the metal (dashed line).

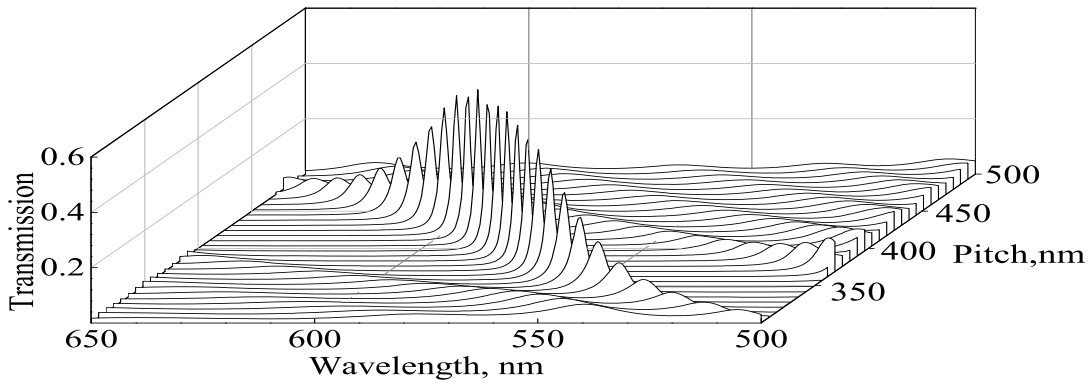

Figure 7. Transmission spectrum of the structure versus cholesteric helix pitch.